Transient Recognition Control for Hybrid Fuel Cell Systems

Tao Zhu, *Member, IEEE*, Steven R. Shaw, *Senior Member, IEEE*, and Steven B. Leeb, *Senior Member, IEEE*

***Abstract*—Hybrid power systems combining fuel cells with fast energy storage devices are good solutions to the fuel cell load-following problem. Hybrid systems may also offer efficiency and reliability advantages. In this paper, we propose a power control scheme for hybrid systems that exploits feed-forward information about the steady-state behavior of incoming load transients. The method uses a modified cluster-weighted modeling (CWM) algorithm to build a load transient recognition model. The model is formulated sequentially and can provide useful feed-forward information in real time. Simulation and experimental results are provided that demonstrate the effectiveness of the transient recognition model and the proposed power control scheme for hybrid fuel cell systems.**

***Index Terms*—Cluster-weighted modeling, fuel cell, hybrid power system, load transient, pattern recognition.**

I. Introduction

FUEL CELLS have attracted much attention as an efficient, scalable, low-pollution means of generating electrical power. Potential fuel cell applications include distributed generation, auxiliary and primary generation in transportation systems, consumer electronics, and backup generation. Load transients often involve significant peaks in power relative to the steady-state load that may impact lifetime and efficiency of fuel cells [1], [2]. The effects of load transients can be reduced by combining fuel cells with energy storage devices such as capacitors or batteries to form a hybrid system as in [3]–[10]. This paper presents a power control scheme using feed-forward information about load transient behavior to manage the flow of energy between components of a hybrid fuel cell system. This control scheme may allow designers to minimize energy storage requirements, improve system reliability, reduce internal loss, and extend the lifetime of fuel cell systems.

Hybrid fuel cell systems have been proposed for improved transient response in several scenarios. Proton exchange membrane (PEM) fuel cells are considered in [3], [6], [8]–[10] in combination with lead-acid batteries, Li-ion batteries, and capacitors as energy storage elements for portable military electronics and communication applications. A fuel cell system coupled with a superconducting magnetic energy storage system (SMES) is proposed in [7] for a distributed generation system. The authors of [4] investigate the combination of a direct methanol fuel cell (DMFC) with an all-solid-state supercapacitor. The authors in [11]–[15] consider combining fuel cells with batteries or super-capacitors for electric vehicle applications.

Simple hybrid fuel cell systems connect the energy storage device in parallel with the fuel cell. During a transient, the portion of current delivered from the fuel cell is determined implicitly by the impedances of the fuel cell and the storage device. An example can be found in [5]. Some hybrid systems control the fuel cell to output approximately constant power as in [3], [6]–[8]. In these applications, the storage device handles all transient energy and the fuel cell operates like a battery charger.

The transient performance of a hybrid fuel cell system can be improved if the control system can determine the future behavior of the transient. The fuel cell can then be controlled to avoid responding to large transient currents. In limited, fixed-load scenarios, it may be possible for an external communications network to alert a hybrid system to the startup behavior of key loads. In this paper, we present a more flexible system motivated by the near real-time transient recognition capabilities of the nonintrusive load monitor (NILM) in [16]. The NILM is capable of disaggregating and recognizing individual loads from a current waveform using a library of transient signatures. The hybrid control problem considered in this paper differs from NILM in that the identification of the long-range transient behavior must happen quickly, on a time-scale shorter than the transient. This paper demonstrates the performance of a fuel cell and battery prototype hybrid system using a low-latency sequential modification of cluster-weighted modeling (CWM) [17]–[19] presented in [20].

Our power controller is developed in the following section for a fuel cell system, but also applies to similar systems with transient-sensitive sources. Section III gives an overview of the sequential CWM method developed in [20] and its use in transient recognition control. The results section demonstrates the capabilities of sequential CWM with experimental results showing the behavior of the power electronics and loads under transient recognition control. A hybrid system with transient recognition control is compared to a simple connection of power electronics to a fuel cell.

Manuscript received July 8, 2004; revised September 17, 2004. This work was supported by the National Science Foundation under Grant ECS-0135229 and the High Temperature Electrochemistry Center (HiTEC), Pacific Northwest National Lab. under Contract 3971 (413030-A). Paper no. TEC-00143-2004.

T. Zhu and S. R. Shaw are with the Department of Electrical and Computer Engineering, Montana State University, Bozeman, MT 59717 USA (e-mail: tzhu@mymail.msu.montana.edu; sshaw@matrix.coe.montana.edu).

S. B. Leeb is with the Department of Electrical Engineering and Computer Science, Massachusetts Institute of Technology, Cambridge, MA 02139 USA (e-mail: sbleeb@mit.edu).

Digital Object Identifier 10.1109/TEC.2005.853785

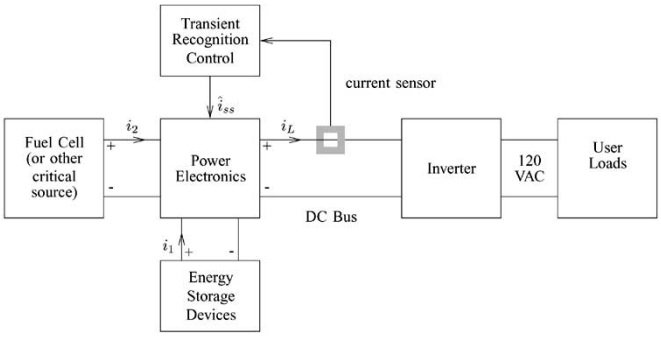

Fig. 1. Hybrid power control scheme combining fuel cells or other critical source with energy storage devices. The current demanded for the fuel cell is determined by the recognition of the load transient. This system shows an inverter and ac load, but dc loads could also be used.

II. Novel Power Control Scheme for Hybrid Fuel Cell Systems

Fig. 1 shows the proposed transient-based control scheme for a hybrid system using energy storage elements and fuel cells or other critical sources. The power electronic circuit in Fig. 1 regulates the voltage on the dc bus and uses the input command from the transient recognition control (TRC) module to adjust energy flow from the storage devices and the fuel cells during a transient. The architecture in Fig. 1 allows the fuel cell to respond to the estimate of the steady-state behavior of the load supplied by the TRC module. In contrast, the response of a conventional control depends on the initial transient behavior. A conventional control may unnecessarily accelerate the reactions in the fuel cell, leading to thermal consequences and system inefficiency. The system in Fig. 1 is particularly useful when the magnitude of the load transients is significant compared to the capacity of the critical source.

Fig. 2 shows the potential advantages of the transient control scheme in Fig. 1. The load current transient on the dc bus, in this case from an incandescent light bulb, has initial values that are large relative to the steady-state value. The "conventional control" response shows how a hybrid system with a linear controller might control the fuel cell for this transient. Storage devices provide the difference between the load current and the fuel cell output current at the beginning of the transient. However, the fuel cell response overshoots the demand before reaching steady state, vigorously accelerating the generating process. In contrast, the transient recognition control response in Fig. 2 shows how the fuel cell could respond to the transient given the estimate of the long-range transient behavior $\hat{i}_{\rm ss}$.

Given a class of transients, a conventional control system could be designed to minimize the overshoot, fuel cell thermal excursions, or any other criterion of interest. However, that control would be a compromise solution over all possible loads. A control that recognizes the "fingerprint" of an incoming load can provide a response that is optimal for that load. The delay in estimating a useful $\hat{i}_{\rm ss}$ must be as short as possible. We address this problem by adopting a sequential modification of cluster-weighted modeling to the hybrid control problem. In practical systems it may be desirable to combine the TRC with some conventional control to handle, for example, small offset errors in $\hat{i}_{\rm ss}$ in the steady state.

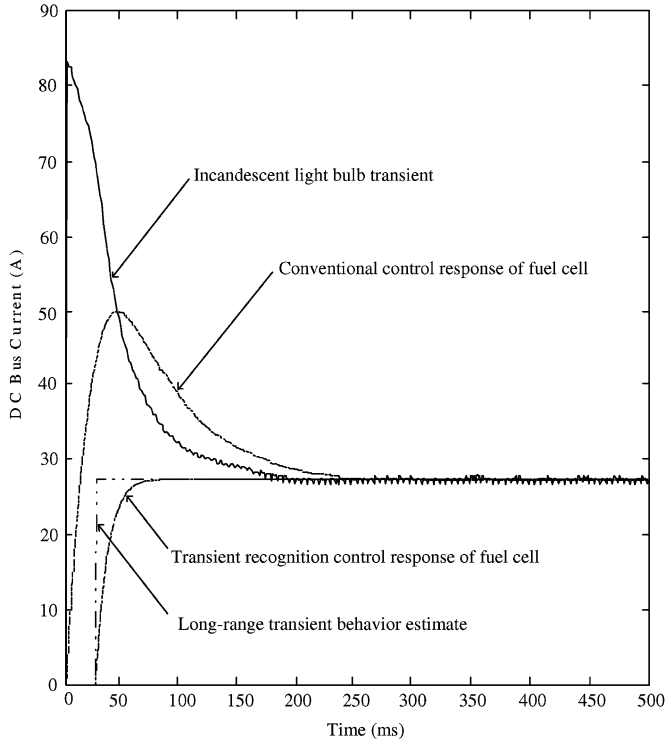

Fig. 2. Theoretical comparison of conventional control and transient recognition control responses to a load transient.

TABLE I
Summary of Key Notation

Notation	Meaning
$\vec{\theta}^{(d1:d2)}$	$(\,\theta_{d1} \quad \cdots \quad \theta_{d2}\,)^T$ for any vector $\vec{\theta}$
$P(c_m)$	prior probability of cluster c_m
$p(\vec{x}_n \mid c_m)$	conditional prior probability density of input $\vec{x}_n$ given cluster c_m representing input pattern space
$p(y_n \mid \vec{x}_n, c_m)$	conditional prior probability density of output y_n given cluster c_m representing input pattern space, and $\vec{x}_n$ the input
$p(c_m \mid y_n, \vec{x}_n)$	conditional posterior probability density of cluster c_m given $\{y_n, \vec{x}_n\}$ being observed
$p(y_n, \vec{x}_n)$	joint probability density of sample pair

III. Sequential Load Transient Recognition

This section provides an overview of our implementation of the transient recognition control using a modification of the cluster weight modeling (CWM) method. We begin with a review of the CWM method using the notation in [18]. Full derivations can be found in [18]. The remainder of the section includes development of a sequential CWM predictor for real-time fuel cell control, a transient scaling scheme, and a description of how the TRC module in Fig. 1 can be implemented. Table I summarizes the notation used in this section.

A. Cluster-Weighted Modeling

Cluster-Weighted Modeling [17]–[19] is an iterative scheme for constructing a functional mapping between input patterns $\vec{x}$ and outputs y given a sample set $\{y_n, \vec{x}_n\}_{n=1}^N$, where N is the total number of samples. CWM characterizes the input space using a number of clusters. Each cluster includes a stochastic description of how the inputs group around the cluster and a local model relating the input to the desired output for that cluster. The output of a CWM is a probabilistic combination of all the cluster outputs, which allows CWM to achieve a globally nonlinear mapping even if the local models are linear. CWM has proven useful for pattern recognition, stochastic time series analysis and synthesis [19], [21], [22], and nonlinear modeling [23].

A cluster c_m in CWM consists of a probability $P(c_m)$ and probability densities $p(\vec{x}_n \mid c_m)$ and $p(y_n \mid \vec{x}_n, c_m)$. The prior probability $P(c_m)$ is a reflection of the relative importance of c_m to the model. If input patterns associated with c_m occur often, $P(c_m)$ is relatively large. The conditional probability density $p(\vec{x}_n \mid c_m)$ can be thought of as the likelihood of the input $\vec{x}_n$ with respect to the cluster c_m. If $\vec{x}_n$ is far from c_m, then $p(\vec{x}_n \mid c_m)$ is small. Finally, the conditional density $p(y_n \mid \vec{x}_n, c_m)$ is the likelihood of a particular output y_n for the c_m cluster, given the input $\vec{x}_n$. For load transient recognition, $\vec{x}_n$ is the input load transient, y_n is the long range behavior of the transient, and a cluster c_m may represent a particular transient or class of transients.

The probability densities in CWM are used to localize the input space, and can be any suitable function. However, Gaussian density models, i.e.,

$$p(\vec{x}_n \mid c_m) = \prod_{d=1}^{D} \frac{1}{\sqrt{2\pi\sigma_{m,d}^2}} \exp\left[\frac{-(x_{n,d} - \mu_{m,d})^2}{2\sigma_{m,d}^2}\right] \quad (1)$$

$$p(y_n \mid \vec{x}_n, c_m) = \frac{1}{\sqrt{2\pi\sigma_{m,y}^2}} \exp\left[\frac{-(y_n - f(\vec{x}_n, \vec{\beta}_m))^2}{2\sigma_{m,y}^2}\right] \quad (2)$$

have an intuitive probabilistic interpretation and good localization properties. In (1), D is the dimension of the transient pattern $\vec{x}_n$. Also in (1), the full covariance matrix is replaced with a variance matrix with D diagonal elements $\sigma_{m,d}^2$. Although the full covariance matrix would allow the CWM to use correlation information, the size and computational costs grow quickly with the length of the transient pattern.

The local model for each cluster, $f(\vec{x}_n, \vec{\beta}_m)$, is embedded in (2) as the expectation value of the conditional output density function. The local model parameters $\vec{\beta}_m$ are determined as a part of the estimate of $p(y_n \mid \vec{x}_n, c_m)$. The global mapping is a "cluster weighted" combination of the local mappings for each cluster. Specifically, the contribution of each local model for each cluster is weighted by a likelihood that the input data is associated with that cluster

$$\begin{aligned}\langle \hat{y} \mid \vec{x}_n \rangle &= \int y \cdot p(y \mid \vec{x}_n) dy \\ &= \frac{\sum_{m=1}^{M} f(\vec{x}_n, \vec{\beta}_m) p(\vec{x}_n \mid c_m) P(c_m)}{\sum_{m=1}^{M} p(\vec{x}_n \mid c_m) P(c_m)}. \end{aligned} \quad (3)$$

In (3), M is the total number of clusters and $p(\vec{x}_n \mid c_m)P(c_m)$ is a likelihood weighted by the prior probability of the cluster c_m. The denominator in (3) is a normalization factor for the weighted combination. Although any output from (3) depends on all clusters for all different loads, the interaction between classes of loads with dissimilar transients is weak. For example, local models formulated for light bulbs will have little influence on outputs associated with motors because $p(\vec{x}_{\text{motor}} \mid c_{\text{bulb}})$ is very small. The models $f(\vec{x}_n, \vec{\beta}_m)$ in (2) can be relatively simple because of the localization properties of $p(\vec{x}_n \mid c_m)$ in (3). We use a linear local model

$$f(\vec{x}_n, \vec{\beta}_m) = \vec{\beta}_m^T \cdot \vec{x}_n = \sum_{d=1}^{D} \beta_{m,d} \cdot x_{n,d}. \quad (4)$$

With this choice of $f(\vec{x}_n, \vec{\beta}_m)$, CWM can be thought of as a bank of FIR filters, each tuned to a particular load transient, with a probabilistic mechanism for selecting an appropriate combination of outputs.

The presentation in this section emphasizes the output prediction process using (3). The output prediction is most critical in the hybrid control scenario because it must be real-time. In contrast, the training or update process for the distributions used in the prediction step can be pseudo real-time. In a given iteration of training, the posterior $p(c_m \mid y_n, \vec{x}_n)$ is evaluated based on the priors $\{P(c_m), p(\vec{x}_n \mid c_m), p(y_n \mid \vec{x}_n, c_m)\}$ from the previous step. Then the posterior is used to update the priors so that they maximize the joint log likelihood $\sum_{n=1}^{N} \log[p(y_n, \vec{x}_n)]$. Refer to [18] for a detailed presentation of CWM training.

B. Sequential CWM Prediction

The CWM estimate (3) of the long range behavior of a load transient requires waiting for a full set of D data points in the input pattern $\vec{x}_n$. This delay may make the resulting estimate useless for the fuel cell system in Fig. 1. The real-time performance of CWM can be improved by a sequential modification of (3) as derived in [20].

The sequential prediction step in [20] splits the vector argument for the local model in (3) into two parts. The first is the K data points just received as input. The second part uses prior information associated with each cluster as a substitute for the missing data. The local model outputs are combined using a cluster weighted sum based on the conditional probabilities for the K received points, i.e.,

$$\langle \hat{y} \mid \vec{x}_n \rangle = \frac{\sum_{m=1}^{M} f(\vec{q}_m, \vec{\beta}_m) p\left(\vec{x}_n^{(1:K)} \,\middle|\, c_m\right) P(c_m)}{\sum_{m=1}^{M} p\left(\vec{x}_n^{(1:K)} \,\middle|\, c_m\right) P(c_m)} \quad (5)$$

where

$$\vec{q}_m = \left(\vec{x}_n^{(1:K)^T} \quad \vec{\mu}_m^{(K+1:D)^T}\right)^T. \quad (6)$$

The vector $\vec{q}_m$ is a reconstruction of the input vector relative to c_m using the K available points from the input and the stored prior information $\vec{\mu}_m^{(K+1:D)^T}$ for the cluster. Some reconstructed input vectors may be rather implausible, such as when the first points of an incoming bulb transient are concatenated with the

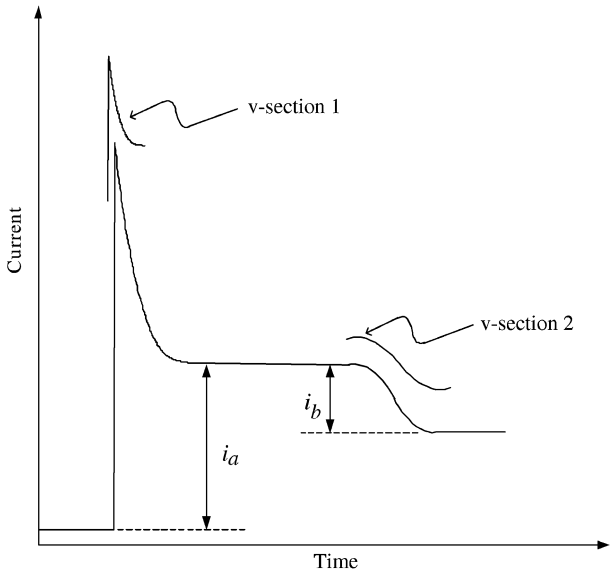

Fig. 3. Informative segments (v-sections) in a load transient. A load transient can have one or more v-sections. Each v-section represents a significant variation in the long-term power dissipation, and can be modeled individually by CWM.

last points of motor transient cluster. However, the likelihood $p(\vec{x}_n^{(1:K)} \mid c_m)$ should be small for reconstructions that join truly dissimilar events. The value of $p(\vec{x}_n^{(1:K)} \mid c_m)$ can be found by taking the product in (1) over K.

C. TRC Implementation

An empirical observation important to the nonintrusive load monitor (NILM) is that transients from differently sized but physically similar loads tend to be similar up to scale factors in amplitude and time [16]. The proposed transient recognition classifier takes advantage of this observation by finding an offset and an amplitude scale factor for the transient relative to the clusters. The offset b is continuously estimated by a moving average filter and is available when the transient arrives. The scale factor a^{ML} for the maximum likelihood cluster is determined sequentially according to the maximum likelihood criterion

$$\max_{a_m, c_m} \log p\left(\tilde{\vec{x}}^{(1:K)} \;\middle|\; c_m, a_m\right) \tag{7}$$

where

$$\tilde{\vec{x}}^{(1:K)} = a_m \cdot \left(\vec{x}^{(1:K)} - b\right). \tag{8}$$

The coefficients a^{ML} and b are then used to prescale the transient before CWM prediction of the associated output. Limits are imposed on the scaling range for each cluster to prevent scaling that is likely to lead to poor results.

In the NILM, the principle purpose of transient recognition is to identify the load. In this context, it is important to apply the same scale factor to each "v-section" or significant feature of the input stream. Fig. 3 shows v-sections in the context of sample transient. In transient recognition control the v-sections can be treated separately. Each v-section is used to predict the effective long range power change. For instance, the first v-section in Fig. 3 can be used to predict the initial change i_a in a long-duration transient. Unlike NILM, there is no need to link v-sections to estimate the exact load type. V-sections are found in the input transient stream by a change of mean detector, as in [16].

A procedure for implementing TRC using sequential CWM is provided here.

Step 1) Filter the input transient signal $\vec{x}^{(1:K)}$ to eliminate switching noise from power electronics.

Step 2) Determine the maximum likelihood scale factor a^{ML}, offset b, and scaled transient data $\tilde{\vec{x}}^{(1:K)}$ as in Section III-C.

Step 3) Compute the partial likelihood $p(\tilde{\vec{x}}^{(1:K)} \mid c_m, a^{\mathrm{ML}})$ for each cluster.

Step 4) Reconstruct the scaled transient vector for each cluster using (6).

Step 5) Calculate $\langle \hat{y} \mid \tilde{\vec{x}}^{(1:K)} \rangle$ according to (5).

Step 6) Apply scale factors to CWM output

$$\hat{i}_{\mathrm{ss}} = \frac{1}{a^{\mathrm{ML}}} \cdot \left\langle \hat{y} \;\middle|\; \tilde{\vec{x}}^{(1:K)} \right\rangle + b. \tag{9}$$

IV. Experimental Results

This section provides two kinds of experimental results. The first set of results shows the application of the sequential cluster-weighted modeling approach to transient recognition control. The results are Matlab simulations of the sequential cluster-weighted model output with measured data as input. The second set of results shows how a real hybrid fuel cell system would react under transient recognition control. These results were obtained by storing the precomputed responses to transients in an arbitrary waveform generator and measuring the system response. The difference between this scenario and a full real-time implementation is that the TRC runs in less than real-time in Matlab. A real-time implementation involves no theoretical changes but technical challenges specific to the choice of platform.

A. Simulation Results

A variety of load transients were collected to test the transient recognition control scheme. The test setup consisted of an HP 6011A power supply operated in constant voltage mode connected to a Xantrex 1750 prowatt inverter. Load transient currents on the dc side of this system were measured using an LEM LA100-P active current sensor connected to a 14-bit data acquisition system. A total of 265 transients were recorded for five types of loads including a lathe, bulb, computer monitor, drill, and vacuum cleaner. The number of transients for each load is indicated in Table II. The monitor transient includes two v-sections that were treated as individual transients.

Measured transients were normalized, FIR filtered to eliminate the 120-Hz ripple from the inverter, and down-sampled. The load transient dimension after down-sampling was $D = 50$. Most of the transients were used to initialize the sequential CWM model, including cluster centers, variances, and local model parameters. More than one cluster was used for each class

TABLE II
CWM CONFIGURATION AND TESTING SPECIFICATIONS

Transient	Training transients	Testing transients	Clusters
Lathe	40	8	6
Monitor v-section1	30	6	6
Monitor v-section2	30	6	6
Bulb	51	17	3
Drill	30	10	3
Vacuum	28	9	3
Total	209	56	27

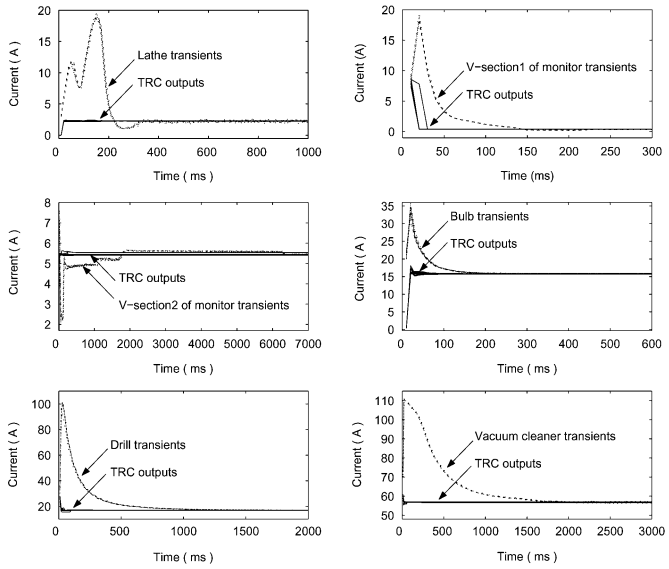

Fig. 4. Testing results of sequential recognition for different load transients.

of transient to accommodate the variability within the class. The last column of Table II shows the number of clusters used for each kind of transient.

A set of 56 measured transients was used to test the CWM. These transients were *not* used for initialization. Although implemented in Matlab, the testing procedure was the same as proposed for real-time TRC implementation.

The TRC prediction results are shown in Fig. 4. The dashed lines show the family of measured transients. The transients show some expected variability between observations. The solid lines show the outputs of the transient recognition control. The TRC outputs have significant prediction errors at the beginning of the transients. This is expected, as it is clearly impossible to determine the future behavior of a transient from the first one or two data points. However, in almost all cases the TRC output settles quickly compared to the length of the transient. In practice a "lock-out" interval could remove spurious low-time TRC outputs to the fuel cell control system.

B. Hybrid Fuel Cell System Results

Fig. 5 shows a diagram of a prototype fuel cell hybrid system built to test the transient recognition control concept. The system in Fig. 5 is a simple representation of the general system in Fig. 1.

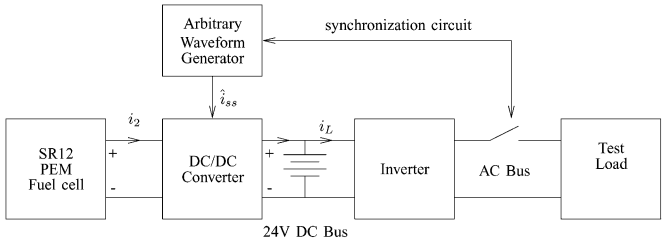

Fig. 5. Multisource test system implementation. This system can be compared to Fig. 1, except that the control signal is synthesized offline and output at the appropriate time by the arbitrary waveform generator.

TABLE III
COMPONENTS USED FOR SYSTEM IN FIG. 5

Component	Specifications
Fuel cell	Avista Labs SR-12 Modular PEM Generator
DC/DC converter	Kollmorgen KXA-80-10-20 PWM servo amplifier
Battery	17 AH, 12V lead acid
DC/AC inverter	EXELTECH XP600 600W Inverter 1100W surge
Arbitrary waveform generator	Tektronix AFG320

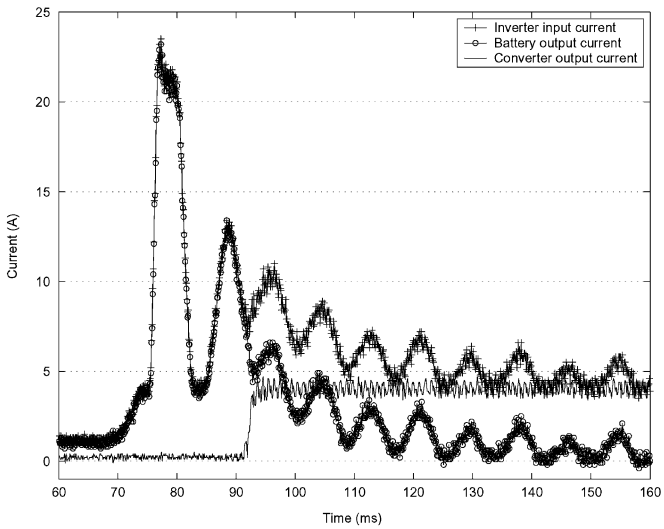

Fig. 6. Responses on dc bus of hybrid fuel cell system to incandescent light bulb transient.

In particular, the battery is connected to the dc bus, providing both voltage regulation and a fast source. The responses of the system in Fig. 5 under TRC are compared to the direct connection of the inverter to the fuel cell without a battery for an incandescent light bulb transient and a lathe transient. A Tektronix TDS3054B oscilloscope and TCP202 current probes were used for all measurements. Other instrumentation details are provided in Table III.

Fig. 6 shows the response of the system to an incandescent light bulb transient. All of the currents in Fig. 6 are on the dc side of the inverter. The load transient starts at about 70 ms. The current is not zero before the transient because the inverter

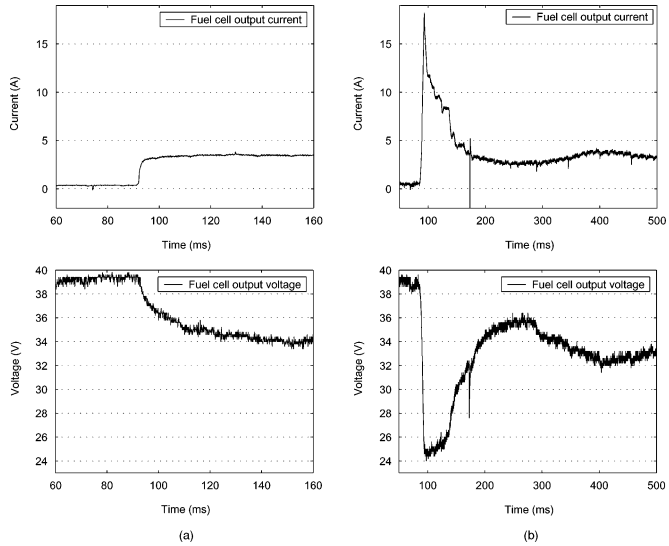

Fig. 7. Responses of hybrid and simple systems to incandescent light bulb transient. (a) Hybrid fuel cell system responses. (b) Direct connection fuel cell system responses.

consumes some power. The current supplied to the inverter is equal to the battery current until about 90 ms, when the TRC control provides an estimate of the steady state current value, which is output from the dc to dc converter. After the fuel cell takes over the load, the battery current drops to an average value of zero. Note that the battery continues to isolate the fuel cell from the ripple of the inverter.

Fig. 7 shows the same incandescent light bulb transient as seen by the fuel cell. The hybrid system responses are on the left. The current from the fuel cell increases at about 90 ms when the dc to dc converter receives the command from the TRC. This step response could be adjusted to meet specific requirements for the fuel cell. The fuel cell voltage in the lower left of Fig. 7 drops in a controlled manner as the load increases. In contrast, the voltage and current responses on the right of Fig. 7 vary greatly and may adversely affect the fuel cell. The peak fuel cell current in response to the light bulb transient reaches nearly 20 A, while the voltage collapses. The transient takes longer to evolve on the graphs to the right because the fuel cell is unable to maintain its output. The steady-state requirement of the light bulb is about 120 W—well within the 500 W rated capacity of the fuel cell and inverter system.

Figs. 8 and 9 show similar results, but for a lathe transient. Fig. 8 shows the simulated TRC response to the lathe transient. The effective recognition time is at 200 ms, when the fuel cell picks up the long range transient requirement. As a result, the fuel cell voltage and current are well-behaved, as shown on the left of Fig. 9. Without TRC there are uncontrolled excursions in voltage and current as seen on the right of Fig. 9. Internal losses in the fuel cell are close to the power delivered for most of the transients on the right side of Fig. 9.

V. Discussion

This paper presents a hybrid fuel cell system control scheme that may improve the reliability, efficiency, and service life of

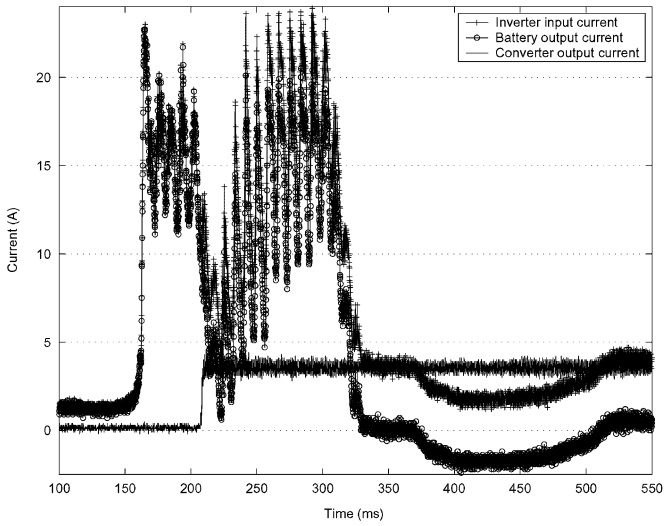

Fig. 8. Responses on dc bus of hybrid fuel cell system to lathe transient.

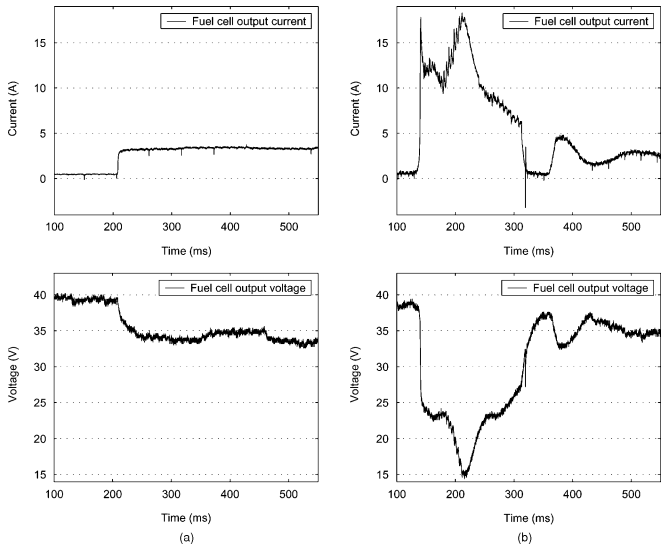

Fig. 9. Responses of hybrid and simple systems to lathe transient. (a) Hybrid fuel cell system responses. (b) Direct connection fuel cell system responses.

fuel cells and other critical sources. The technique is demonstrated by simulation of the proposed method in Matlab using measured transient data and by emulation of a real-time control using an arbitrary waveform generator in a real hybrid system. A real-time implementation is feasible. On-going work includes implementing the TRC in a real-time DSP or FPGA system. If implemented in real-time, the methods in this paper can protect fuel cells from undesirable load transient currents.

The training process for the TRC in this paper was performed once, prior to testing the prediction steps. In practice the training can occur in near real time to adapt the control to new loads. It may be that a generic initialization can be performed for standard loads before installation. Some combination of on-site and off-site initialization may be desirable. The response of sequential CWM to new and overlapping transients is considered in [20]. An advantage of CWM is that "off training set" inputs are easy

to detect by examining the likelihood of the input relative to the clusters. The likelihood of the input can also be used to detect and resolve overlapping transients, a feature that may be useful in NILM applications.

Experimental results suggest that the effective recognition delay of the TRC is significantly less than the pattern length. We found that the TRC typically provides good estimates using about one-fifth of the stored pattern length. Computational effort increases with the pattern length, so it is tempting to explore shorter patterns. We expect to see a tradeoff between shorter patterns and robustness.

REFERENCES

[1] R. S. Gemmen, "Analysis for the effect of inverter ripple current on fuel cell operating condition," *Trans. ASME, J. Fluids Eng.*, vol. 125, pp. 576–585, May 2003.

[2] K. Acharya, S. K. Mazumder, and P. K. Burra, "System interaction analyses of solid oxide fuel cell(sofc) power conditioning system," in *Proc. IEEE Ind. Appl. Conf., 38th IAS Annu. Meeting*, Oct. 2003, pp. 2026–2032.

[3] L. P. Jarvis, T. B. Atwater, and P. J. Cygan, "Fuel cell/electrochemical capacitor hybrid for intermittent high power applications," *J. Power Sources*, vol. 79, pp. 60–63, 1999.

[4] K. W. Park, H. J. Ahn, and Y. E. Sung, "All-solid-state supercapacitor using a nafion polymer membrane and its hybridization with a direct methanol fuel cell," *J. Power Sources*, vol. 109, pp. 500–506, 2002.

[5] J. C. Amphlett, E. H. de Oliveira, R. F. Mann, P. R. Roberge, A. Rodrigues, and J. P. Salvador, "Dynamic interaction of a proton exchange membrane fuel cell and a lead-acid battery," *J. Power Sources*, vol. 65, pp. 173–178, 1997.

[6] P. B. Jones, J. B. Lakeman, G. O. Mepsted, and J. M. Moore, "A hybrid power source for pulse power applications," *J. Power Sources*, vol. 80, pp. 242–247, 1999.

[7] R. Nojima, I. Takano, and Y. Sawada, "Transient performance of a new-type hybrid electric power distribution system with fuel cell and SMES," in *Proc. IECON'01, 27th Annu. Conf. IEEE Ind. Electron. Society*, 2001, pp. 1303–1308.

[8] L. P. Jarvis, P. J. Cygan, and M. P. Roberts, "Hybrid power source for manportable applications," *IEEE Aerosp. Electron. Syst. Mag.*, vol. 18, pp. 13–16, Jan. 2003.

[9] L. P. Jarvis, T. B. Atwater, E. J. Plichta, and P. J. Cygan, "Power assisted fuel cell," *J. Power Sources*, vol. 70, pp. 253–257, 1998.

[10] L. P. Jarvis, T. B. Atwater, and P. J. Cygan, "Hybrid power sources for land warrior scenario," *IEEE Aerosp. Electron. Syst. Mag.*, vol. 15, pp. 37–41, Sep. 2000.

[11] L. U. Gokdere, K. Benlyazid, R. A. Dougal, E. Santi, and C. W. Brice, "A virtual prototype for a hybrid electric vehicle," *Mechatronics*, vol. 12, pp. 575–593, 2002.

[12] H. S. Lee, K. S. Jeong, and B. S. Oh, "An experimental study of controlling strategies and drive forces for hydrogen fuel cell hybrid vehicles," *Int. J. Hydrogen Energy*, vol. 28, pp. 215–222, 2003.

[13] K. S. Jeong and B. S. Oh, "Fuel economy and life-cycle cost analysis of a fuel cell hybrid vehicle," *J. Power Sources*, vol. 105, pp. 58–65, 2002.

[14] L. Bertoni, H. Gualous, D. Bouquain, D. Hissel, M. C. Pera, and J. M. Kauffmann, "Hybrid auxiliary power unit (apu) for automotive applications," in *Proc. Vehicular Technology Conf. 2002. VTC 2002-Fall*, Sep. 2002, pp. 1840–1845.

[15] M. Nadal and F. Barbir, "Development of a hybrid fuel cell/battery powered electric vehicle," *Int. J. Hydrogen Energy*, vol. 21, no. 6, pp. 497–505, 1996.

[16] S. R. Shaw, "System Identification Techniques and Modeling for Non-Intrusive Load diagnostics," Ph.D. dissertation, MIT, Cambridge, MA, Feb. 2000.

[17] N. Gershenfeld, B. Schoner, and E. Metois, "Cluster weighted modeling for time-series analysis," *Nature*, vol. 397, pp. 329–332, Jan. 1999.

[18] N. Gershenfeld, *The Nature of Mathematical Modeling*. Cambridge, U.K.: Cambridge Univ. Press, 1999.

[19] B. Schoner and N. Gershenfeld, "Cluster-weighted modeling: Probabilistic time series prediction, characterization and synthesis," in *Nonlinear Dynamics and Statistics*, A. Mees, Ed. Boston, MA: Birkhäuser, 2001, pp. 365–385.

[20] T. Zhu, S. R. Shaw, and S. B. Leeb, "Sequential cluster weighted modeling for electric load transient recognition," unpublished.

[21] B. Schoner, C. Cooper, C. Douglas, and N. Gershenfeld, "Data-driven modeling and synthesis of acoustical instruments," in *Proc. Int. Computer Music Conf.*, Ann Arbor, MI, Oct. 1998.

[22] B. Schoner, C. Cooper, and N. Gershenfeld, "Cluster-weighted sampling for synthesis and cross-synthesis of violin family instruments," in *Proc. Int. Computer Music Conf.*, Berlin, Germany, Aug. 2000.

[23] B. Schoner and N. Gershenfeld, "Data-driven modeling of nonlinear microwave devices," in *Dig. 53rd ARFTG Conf. Nonlinearity Characterization*, Anaheim, CA, Jun. 1999.

Tao Zhu (M'01) received the B.E. and M.E. degrees in 1996 and 1999, respectively, both from Tianjin University, China. He is now a graduate student in the Electrical and Computer Engineering Department, Montana State University, Bozeman.

He is interested in signal processing, pattern recognition, and system identification.

Steven R. Shaw (S'97–SM'05) received the Ph.D. degree in electrical engineering from the Massachusetts Institute of Technology, Cambridge, in 2000.

He is currently an Assistant Professor in the Department of Electrical and Computer Engineering at Montana State University, Bozeman. He is interested in sensors, instrumentation, modeling, numerical and computational methods associated with control, and measurement problems.

Steven B. Leeb (S'89–M'91–SM'01) received the Ph.D. degree in electrical engineering and computer science from the Massachusetts Institute of Technology (MIT), Cambridge, in 1993.

He has been a member of the M.I.T. faculty in the Department of Electrical Engineering and Computer Science since 1993. He currently serves as an Associate Professor in the Laboratory for Electromagnetic and Electronic Systems. He is concerned with the design, analysis, development, and maintenance processes for all kinds of machinery with electrical actuators, sensors, or power electronic drives.